

Article

Investigation of the Corrosion and Tribological Properties of WC-Co Tools Hardened with PVD Coatings in Solid Oak Wood Processing

Deividas Kazlauskas ^{1,*}, Vytenis Jankauskas ¹  and Maksim Antonov ² ¹ Agriculture Academy, Vytautas Magnus University, 53361 Kaunas, Lithuania; vytenis.jankauskas@vdu.lt² Department of Mechanical and Industrial Engineering, Tallinn University of Technology, 19086 Tallinn, Estonia; maksim.antonov@taltech.ee

* Correspondence: deividas.kazlauskas@vdu.lt; Tel.: +370-605-58167

Abstract: Corrosion and friction coefficient tests were performed on solid oak wood machined with hard-metal woodworking tools coated with PVD coatings (AlCrN, AlTiN, TiAlN, TiCN and CrN). The tannic acid attacks the carbide more intensively than the PVD coatings. During cutting, corrosion spreads on the cutting edge of the cutter due to mechanical action, which dissolves the cobalt binder of the hard-metal and causes the carbide grains to flake off. After 80 min of contact with the wood, the cobalt content decreases from 3.53 to 1.74%. Depending on the PVD coating material, cracks of 4 to 40 μm in width appear after 120 min (9000 m cutting path). After 120 min of machining, wear, corrosion effects and the influence of corrosion on the coefficients of friction were evaluated for tools with and without PVD coatings. TiCN is the most sensitive to corrosion, while AlCrN and CrN coatings are the least sensitive, with the AlTiN coating being the most affected under real cutting conditions (with mechanical + thermal + corrosion effects) and the tools with CrN and AlCrN coatings being the least affected. Corrosion affects the hard-metal and PVD coatings and reduces the coefficient of friction. The angle between the directions of sliding and sharpening of the cutting edge sharpening significantly influences this parameter. The coefficient of friction of hard-metal WC-Co and PVD coatings is higher in the parallel machining direction than in the perpendicular machining direction and ranges from 16.03% (WC-Co) to 44.8% (AlTiN). The coefficient of friction of hard-metal WC-Co decreases by 5.13% before and after exposure to tannic acid, while the corrosion of PVD coatings reduces it by 4.13% (CrN) to 26.7% (TiAlN).

Keywords: PVD coatings; oak wood; wood cutting; hard metal; corrosion; tannins



Citation: Kazlauskas, D.; Jankauskas, V.; Antonov, M. Investigation of the Corrosion and Tribological Properties of WC-Co Tools Hardened with PVD Coatings in Solid Oak Wood Processing. *Coatings* **2024**, *14*, 569. <https://doi.org/10.3390/coatings14050569>

Academic Editor: Alina Vladescu

Received: 30 March 2024

Revised: 19 April 2024

Accepted: 30 April 2024

Published: 3 May 2024



Copyright: © 2024 by the authors. Licensee MDPI, Basel, Switzerland. This article is an open access article distributed under the terms and conditions of the Creative Commons Attribution (CC BY) license (<https://creativecommons.org/licenses/by/4.0/>).

1. Introduction

Trees are important for people's lives and activities: they protect the soil and stabilize the climate, they offer social benefits and provide raw materials for the construction and furniture industries. Wood is an important renewable natural resource that stores carbon by absorbing CO₂ from the atmosphere. The anatomy of wood influences its physical and mechanical properties [1–8]. Wood is an inhomogeneous, anisotropic, fibrous plant material. It consists of a rigid, coherent framework of densely packed hollow cells whose cavities are filled with air or water. About 99% of the total dry weight of wood consists of organic and the rest of inorganic substances. The amount and proportion of these substances depends on the type of wood, its age and the growing conditions. The organic substance of wood in its completely dry state contains 49%–50% C, 43%–44% O₂, about 6% H₂ and 0.1%–0.3% N, regardless of the type of wood. Carbon, hydrogen and oxygen form the complex organic substances cellulose, lignin, hemicellulose and extractives. The density of wood is in the range of 0.15–1.09 g/cm³ [9–12]. The structure of wood is shown in Figure 1.

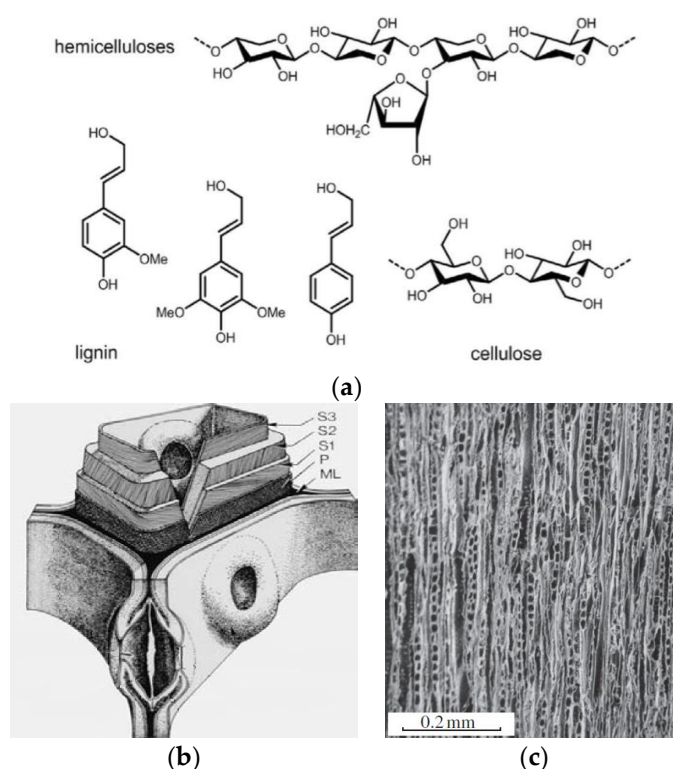


Figure 1. Structural composition and structure of wood: (a) structure of cellulose, lignin and hemicellulose molecules; (b) structure of the cell wall; (c) longitudinal section of oak wood [11,13,14].

Wood contains more than 700 different extractive substances, some of which affect the corrosion of metals in contact with wood or pulp solutions. These include organic acids (acetic acid and formic acid), tannins (polyphenols) and phenols with two or three neighboring hydroxyl groups (catechol and pyrogallol). The concentration of extractives in wood varies between 1.4 and 13.8% [15,16].

Wood extracts have been shown to act as lubricants and effectively reduce the coefficient of friction during cutting. However, many studies have also shown that wood extracts (gums, fats, resins, sugars, starch, alkaloids and tannins) have a negative effect on cutting tools [17,18].

Wood species with a lower pH value have a higher corrosive activity [15], but a tannic acid solution in water is the most aggressive [19,20]. Therefore, the wetter the wood is during machining, the more active abrasive and corrosive wear will be [21].

Corrosion also affects unused tools if they are coated with residues of extraction agents. The corrosion of cutting tools is influenced by: the type of wood, the humidity of the wood and the air, the operating temperature of the tool, the age of the wood and the duration of exposure to the active substances [19,20].

Studies in the pulp industry show that tannins inhibit corrosion. Wood tannins are used as metal primers or corrosion inhibitors. Under the action of tannins, the polyphenol complex interacts with metal ions and forms insoluble surface metal tannates (a dark blue/purple mass). During cutting, the iron tannates are removed from the tool surface by the friction and/or temperature of the chip. This exposes new surfaces to corrosion, but if they are already present on the surface, they protect the metal. At certain pH values, the tannins inhibit the corrosion caused by wood extracts [15].

In general, the effect of tannins on the corrosion of tool materials in contact with solid wood has not been studied in detail. Solid wood and its composites are intensively machined and the tools are subject to heavy wear, which affects the cost of machining. Understanding the corrosion and wear behavior of wood cutting tools helps in the selection of cutting materials for machining wood and wood composites.

Wood cutting is a tribological process accompanied by high contact pressure on the tool surface, sliding speeds of up to 40 ms^{-1} , temperatures of up to $900 \text{ }^\circ\text{C}$, the moisture content of the wood and chemical attack. It is known that tool corrosion reduces the friction between the tool and the chip to be cut, i.e., making the cutting process easier [11,15,22].

The increase in the use of hard-coated tools in woodworking is illustrated by the increase in the number of articles in the Science Direct database between 2000 and 2023, as shown in Figure 2. Search terms woodworking, tool, hard coatings.

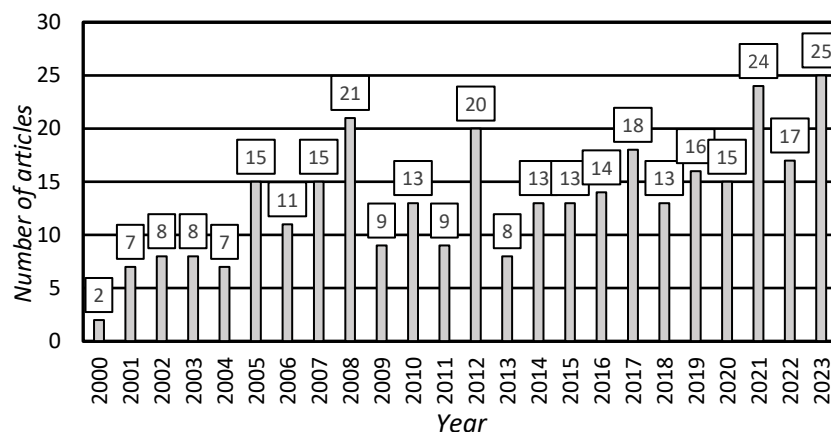


Figure 2. Dynamics of the number of publications on PVD-coated woodworking tools from 2000 to 2023 (Science Direct database).

Hard PVD coatings are widely used in various industrial sectors, including to reduce tool wear [23–29], but the effect of tannic acids on these coatings has not yet been investigated.

Aim: Application of anticorrosive and mechanical/abrasive wear properties of PVD coatings in the treatment of oak wood exposed to intense tannic acid corrosion. Find coatings with higher durability, which would facilitate the cutting process by reducing tool expenses, minimizing equipment downtime when changing tools, and streamlining their adjustment.

Objective:

1. Wear tests on milling cutters without and with PVD coatings for milling solid oak wood;
2. Investigation of the effect of dressing the cutters on the variation of element concentrations on the cutter rake face;
3. Corrosion studies of PVD coatings in aqueous tannic acid solution at different temperatures;
4. Measurement of static and dynamic friction coefficients for new and corroded WC-Co tools without and with PVD coatings.

2. Materials and Methods

The object of the research is the WC-Co (Co 6%) hard-metal (Co 6%) $30 \times 12 \times 1.5 \text{ mm}$ double-edge cutters for woodworking (Figure 3a). Manufacturer: TIGRA GmbH, material: T06MG (Table 1). The cutters were coated with micrometre-thick PVD coatings (AlCrN, AlTiN, TiAlN, TiCN and CrN) by Oerlikon Balzers Coating AG (Balzers, Liechtenstein) and CemeCon Scandinavia A/S (Hinnerup, Denmark). The coatings AlCrN, AlTiN, TiAlN and CrN are single-layer coatings and TiCN is multi-layer. The TiCN coating structure is described in sources [30,31].

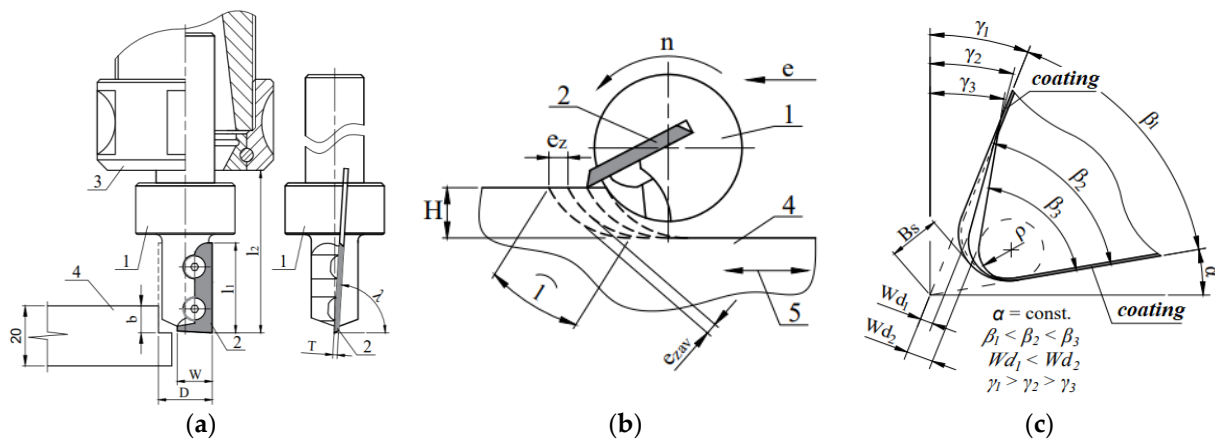


Figure 3. Milling tool and milling scheme: (a) milling tool; 1—fixed tool; 2—cutter; 3—HSK 63F gripper; (b) milling scheme: 1—milling tool; 2—cutter; 4—oak wood; 5—wood fiber direction; H—thickness of the layer to be milled; e_z —feed per one cutter; e—feed direction; n—direction of rotation of the cutter; l—length of the contact arc (chip length); e_{zav} —average chip thickness; (c) α —clearance angle; β —blade angle; γ —rake angle; Wd —rake surface wear; B_s —shortening of the blade; ρ —rounding radius of the cutting edge.

Coatings based on Ti and Cr are chosen for their tribological properties and wide industrial usage [27,29,32,33].

The physical/mechanical properties of WC-Co hard-metal cutters are given in Table 1 [34].

Table 1. Type (composition), physical/mechanical properties of WC-Co hard-metal [34].

Type of Hardmetal	Binder Co, %	WC Grain Size, μm	Hardness, HV 10	Bending Strength, N/mm^2	Tensile Strength, K1C/MPa m-1/2	Max. Operating Temperature, $^\circ\text{C}$	Coefficient of Friction
T06MG	6	0.7–1.0	1800	2700	8.4	800–1000	0.4–0.6

Average microhardness of PVD Coatings, GPa: AlCrN— 27.6 ± 3 GPa, AlTiN— 29.8 ± 3 , TiAlN— 30.8 ± 4 , TiCN— 31.3 ± 3 , CrN— 19.4 ± 2 [35].

Structural composition of the hard-metal cutters and their coatings measured by XRD on a Bruker D8 spectrometer with Cu $K\alpha$ X-ray tube [35].

Cutting tool wear and corrosion of wood were assessed by milling polyvinyl acetate dispersion adhesive glued solid oak (*Quercus Robur*) wood panels ($1000 \times 1000 \times 20$ mm). The wood has an average moisture content of $\omega = 8\%$, an average annual rings density of 4.6 cm^{-1} , and a density of $\rho = 738 \text{ kg/m}^3$. The milling tool and the milling scheme are illustrated in Figure 3a–c. The cutter tests were carried out with a milling cutter with a single interchangeable cutter. Machining conditions: ambient temperature $19 \pm 2 \text{ }^\circ\text{C}$, relative humidity $60\% \pm 5\%$. Milling until the cutting path reaches 9000 m (2.15 million cycles with a chip length of 4.2 mm per cycle— l_{chip}).

The cutting test was carried out at cutting path intervals of 1000, 2000, 3000, 6000 and 9000 m. The values of working time corresponding to these values are 13.3, 26.7, 40, 80 and 120 min, respectively.

The characteristics of the milling tool are given in Table 2 and the milling modes in Table 3. The milling machine used was a CNC machining center ProMaster 7123 (Holz-Her GmbH, Nürtingen, Germany).

Table 2. Milling tool characteristics.

Cutter Diameter D, mm	Length of Tool Fitted, l_2 , mm	Rake Angle γ , °	Sharpening Angle β , °	Clearance Angle α , °	Cutting Angle λ , °
Ø18	55	27	53	10	87

Table 3. Milling mode.

Cutter Rotation Frequency n , 10^3 min^{-1}	Cutting Speed v , ms^{-1}	Thickness of the Layer to Be cut H , mm	Cutter Feed u_z , mm	Contact Arc Length l , mm	Average Chip Thickness e_{zav} , mm	Width of Cut Layer, mm
18	17	1.0	0.1	4.2	0.024	6.0

A 50 mL solution of 5% by weight of tannic acid $C_{76}H_{52}O_{46}$ in water (Carl Roth GmbH + Co., Karlsruhe, Germany) was used for the corrosion test. $C_{76}H_{52}O_{46}$ composition: purity $\geq 95\%$, moisture $\leq 7\%$, impurities: dextrin, rubber, salts, disaccharide, sulphate minerals $\leq 0.1\%$.

The corrosion of the cutters was carried out in a SYSTEC VE-40 autoclave (Systec GmbH & Co. KG, Osnabrück, Germany) at 20, 80 and 140 °C. At 140 °C, the test was carried out at an autoclave pressure of 0.4 MPa (Figure 4) [19]. The visual corrosion effects on the surface of the cutters were recorded four times at 4-h intervals (up to 16 h) using an Eclipse MA-100 metallographic microscope (Nikon Instruments Inc., Melville, NY, USA).

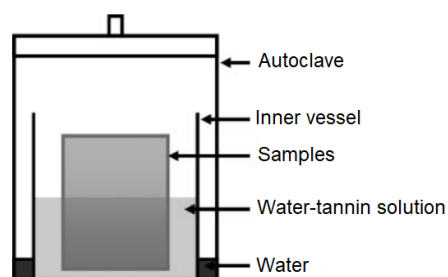


Figure 4. Principle diagram of a corrosion study [19].

Corrosion testing was selected after analyzing the real working conditions of the cutters (environment and temperature) and considering the corrosion testing standards such as ASTM D1141-98, G 1, G 15, G28-22, G 46, G 107, G 48-00, and others. As a result, the evaluation of corrosion damage was performed using the method of assessing the damaged surface area according to standard ISO 4628-3.

After the corrosion test, the blades were washed in Sonorex Super RK ultrasonic washer (Bandelin electronix GmbH & Co., Berlin, Germany) with distilled water for 30 min to remove any residual acid residue left after draining. After washing, the blades were dried with a dry compressed air jet at 10 bar pressure.

The pH of the tannin-water solution used for corrosion testing was measured with a Hana Combo Hi-98130 (Dynamic Aqua-Supply, Surrey, BC, Canada).

The change in the chemical composition of PVD coating surfaces under the influence of tannic acid was determined by EDS analysis using a Hitachi S-3400N-II SEM (Hitachi, Tokyo, Japan) and an EDS XFlash 5040 QUAD X-ray energy dispersive spectroscope (Bruker nano GmbH, Berlin, Germany). The SEM Hitachi S-3400N-II was also used for the determination of the thickness of the hard coatings and for the assessment of the tool wear level.

The static coefficient of friction was determined using an inclined plane with WC-Co hard-metal cutters (without and with PVD coatings) embedded in the supports. The blades are fitted with $120 \times 75 \times 40$ mm solid oak wood blocks with different direction of annual rings (cross section, radial section, tangent section). A screw mechanism at a speed of

5 degrees per minute (degree min^{-1}) is used to force the plane until the cutter starts to slide on the surface of wood grain. The angle of inclination of the plane is measured by electronic digital inclinometer angle meter tester LM320B with magnetic surfaces (UNI-T, China).

A Rockwell indenter was used to determine the friction coefficient between the indenter and new and corroded WC-Co and PVD coatings using the CETR/Bruker UMT-2 (Bruker, Billerica, MA, USA). The test was carried out in two directions, perpendicular and parallel to the machining (grinding) direction of the tool. The length of the scratching section is 7 mm, speed 2.33 mm/min. The load used was 4.905 N, which is mechanically non-damaging to the hard-metal and PVD coatings.

3. Results

The XRD results of the cutters (without and with PVD hard coatings) are shown in Figure 5. The XRD spectra of the samples without and with PVD coatings are dominated by the cutter material (WC-Co), with five angular peaks at 2θ (31.53° , 35.62° , 48.37° , 64.08° and 65.89°).

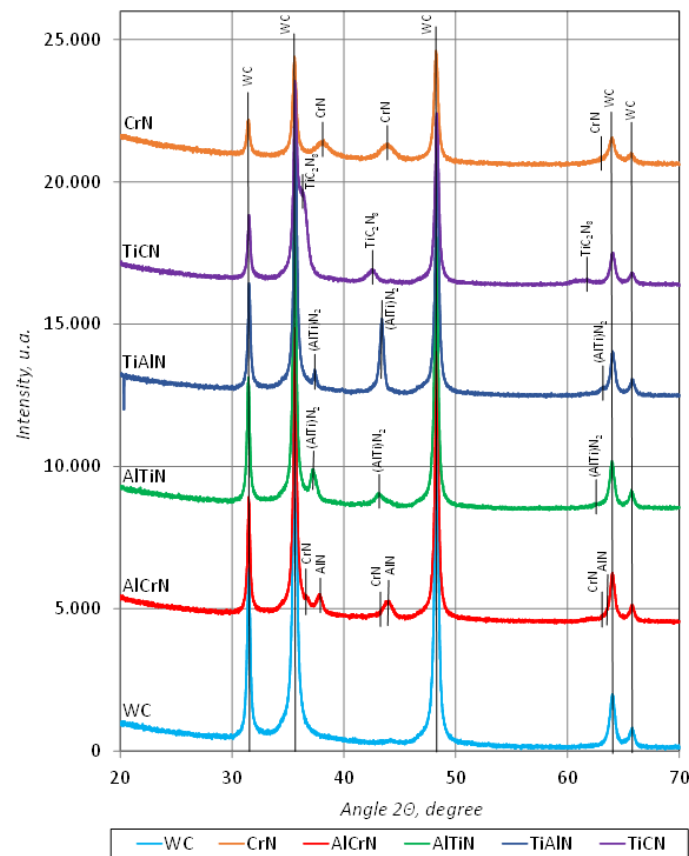


Figure 5. XRD spectra of a solidified sample (WC-Co) and PVD samples coated with AlCrN, AlTiN, TiAlN, TiCN and CrN coatings [34].

Registration of hard-metal WC-Co peaks in XRD spectra in the presence of PVD coatings confirms the micrometric thickness of the coatings. Characteristic peaks in the spectra of PVD-coated cutters at 2θ angles: CrN (37.73° and 44.23°); AlCrN: (AlN— 37.95° , 43.95° , 63.9° and CrN— 44.16°); AlTiN (37.22° , 43.23° , 62.75°); TiAlN (37.40° , 43.41° ; 62.95°); TiCN (36.71° , 42.76° , 61.82°) [35].

XRD measurements of the surface composition of the cutters after the corrosion tests did not show any change in the XRD spectra, i.e., the spectra are identical to those shown in Figure 5. The reason for this is the extremely thin layer of corrosion products not detectable by XRD.

SEM analysis of the fractures of the cutters showed the average thicknesses of the PVD coatings tested to be 1.4 μm for the AlCrN and AlTiN coatings and 2.0 μm for the other coatings (TiAlN, TiCN and CrN) [25].

3.1. Study on Mechanical-Corrosive Effects of Cutting (Cutting Study)

In a study where the wood was cut at a cutter feed rate of 0.1 mm/rev, the PVD coatings did not show any signs of wear on the rake surface wider than 55–60 μm and the full width of the coating wear to the hard-metal substrate did not exceed 40 μm (AlTiN).

SEM analysis of all WC-Co blades with a cutting length of 9000 m (or 120 min running time) when cutting oak wood showed that many of the tungsten carbide grains on the rake surface of the cutter did not have the cobalt (matrix) that binds the grains together (Figure 6a). The surface layers of the WC grains are frayed. This is the result of corrosion by wood extracts, especially tannins [15], which are activated by the operating temperature of the cutting tool.

In PVD-coated cutters with 9000 m of cutting path, all PVD coatings on the cutting edge were damaged (complete delamination). The size of the damage in the cutting edge zone varied from 4 to 40 μm . This was influenced by the mechanical (abrasive) and corrosive resistance of the coating as well as the thickness.

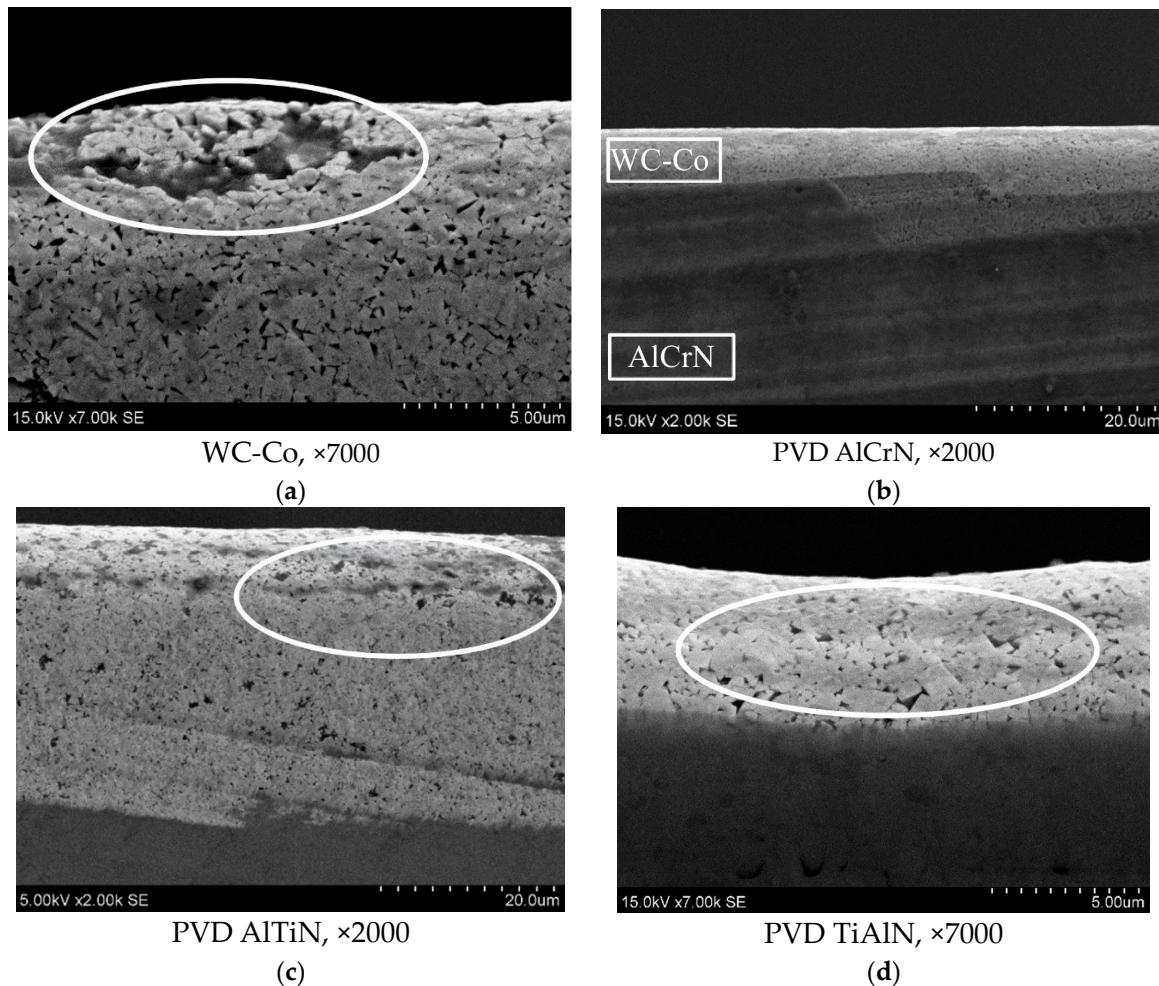


Figure 6. Cont.

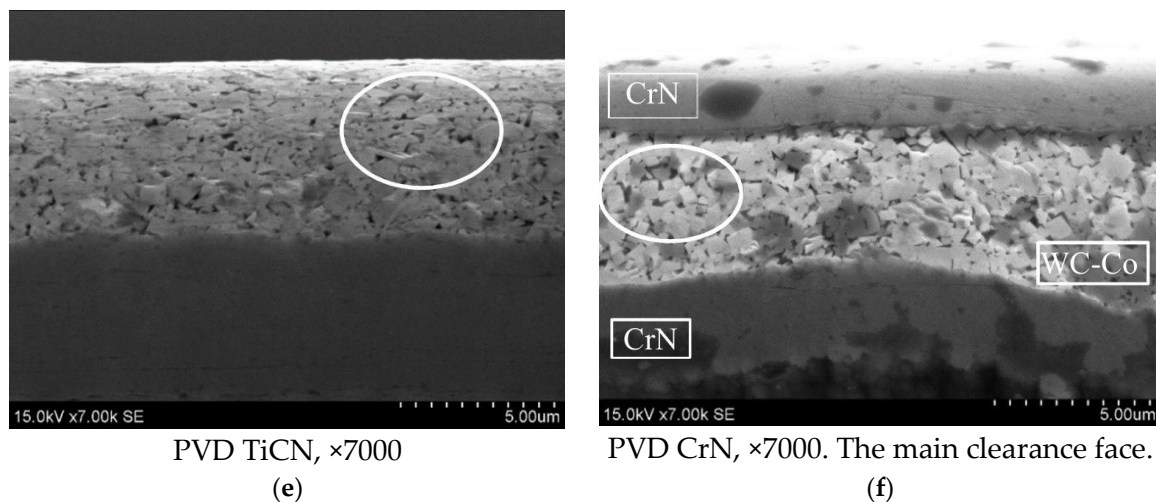


Figure 6. Corroded rake surfaces of uncoated WC-Co (a) and PVD-coated (b–e) cutters after 120 min. cutting time: (a) WC-Co; (b) AlCrN; (c) AlTiN; (d) TiAlN; (e) TiCN; (f) CrN (main clearance face). Cutting edge of the cutters at the top of the illustrations. In order to show the full worn width of the cutting edge, different magnifications ($\times 2000$ and $\times 7000$) are shown.

The uncoated milling cutters (Figure 6a) exhibited the highest corrosion damage (grain degradation), as the hard-metal WC-Co was exposed to mechanical, thermal and corrosive loads for the longest time (120 min). In a study where the wood was cut at a feed rate of 0.1 mm/rev, the PVD coatings showed no signs of wear on the rake surface wider than 55–60 μm , and the total width of wear of the coating on the hard-metal substrate did not exceed 40 μm (AlTiN).

Mechanical/abrasive and corrosive wear caused by the heating of the tool is most active on the cutting edge and rake face of the cutter, where the coating wears fastest. Since the duration of the wood cutting test is the same (120 min), the hard-metal WC-Co tool without PVD coating is most affected (Figure 6a):

- Figure 6a. The abundant hard-metal WC-Co grains (WC) in the surface layers are removed by the Co-corrosion (white oval). Maximum observed corrosion damage (cutting edge of a cutter exposed to corrosion and mechanical stress for 120 min), $\times 7000$;
- Figure 6b: The different wear widths of the coating (6–10 μm) indicate the presence of different coating thicknesses influenced by the roughness of the substrate (AlCrN) during the coating process, $\times 2000$;
- Figure 6c. Wear of the 26–40 μm AlTiN PVD coating, $\times 2000$. This is the highest wear observed in the study.
- Figure 6d: The TiAlN coating on the rake face of the tool is worn away by 5–7 μm (intergranular voids/corrosion in the white oval), $\times 7000$;
- Figure 6e. TiCN coating. Width of the coating wear at the cutting edge approx. 8 μm . Intergranular corrosion of the hard-metal WC-Co on the tool base caused by wear of the coating, shown in the white oval, $\times 7000$;
- Figure 6f. Penetration of a 4–5 μm wide strip of the CrN coating along the cutting edge. Significant intercrystalline cobalt corrosion (cracks between the grains of the solid WC, white oval), $\times 7000$.

The less abrasion-resistant a coating is, the faster it wears off. In this case, the following applies for a fixed test duration: the less wear resistant the PVD coating is, the longer the WC-Co substrate is exposed to corrosion. The mechanical-corrosive effect of the uncoated WC-Co tool lasts for a longer period of time (9000 m of cutting path or ~9 min. of cutting or 120 min. of running time), which leads to the highest cutting edge wear for these tools, Figure 6a. The effect of the PVD coated tools on the substrate of the WC-Co tool only starts after the coating has worn off and the corrosive effects are proportionally lower.

For this reason, the “thinning” of the hard-metal grain spaces is most intense at the cutting edge of the uncoated WC-Co tool. WC is more resistant to corrosion and the binder/matrix cobalt is more susceptible [15,36]. This is clearly shown in Figure 6a. Due to the high wear resistance of the CrN coating [25,31], the coating will only degrade between 4 and 4.5 μm at the cutting edge during the evaluated tool life (Figure 6f). However, if the lower thickness of the AlCrN coating of 1.4 μm and the proportionally higher wear (6–10 μm) are taken into account, it is clear that the mechanical wear resistance of these coatings is equivalent.

According to optical microscopy, the coated tools had the following working distances before the PVD coating wore off: for CrN and AlCrN 6000 m; for TiCN and TiAlN 3000 m; for AlTiN 2000 m.

Since the CrN coating exhibited the least wear, and the wear started later than the other coatings, the corrosive effect of the wood extracts on the solidification was also the lowest. However, even in this case, WC-Co grains can be seen at the location of the worn coating, where the cobalt is not bonded to the adjacent grains, but empty spaces can be seen (Figure 6f).

The cobalt and other elements on the surface of the uncoated hard-metal were analyzed every 3000 m of the cutting path using EDS analysis. The results are presented in Table 4 and Figure 7.

Table 4. Effect of WC-Co cutter output on the elemental content (mass %) of the tool solid.

Cutting Distance, m/Working Time, min	Carbon (C)	Tungsten (W)	Cobalt (Co)	Oxygen (O ₂)	Aluminium (Al)	Chromium (Cr)
0/0	13.48	78.4	3.53	2.96	0.64	0.98
3000/40	13.29	79.4	2.99	3.1	0.41	0.81
6000/80	11.77	77.7	1.74	7.64	0.39	0.74
9000/120	6.53	87.7	3.23	1.28	0.42	0.82

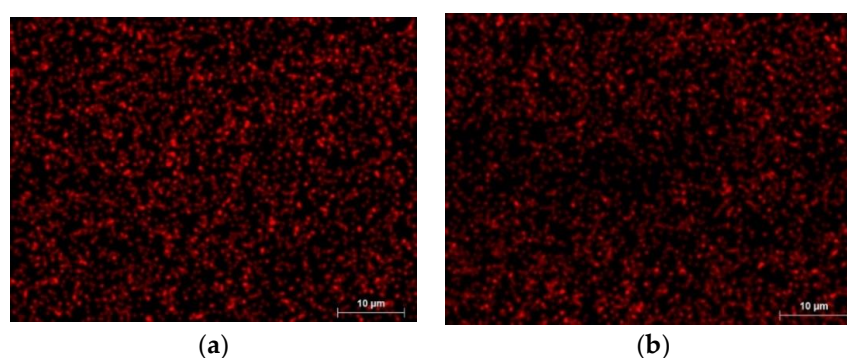


Figure 7. Cobalt distribution on the surface of an EDS hard-metal (WC-Co) cutter, where: (a) L = 0 m; Co—3.53%; (b) L = 6000 m, Co—1.74%; [35].

The low variation in the concentration of elements (C, W, Co, O₂, Cr) at 3000 m cutting distance indicates that no major changes have taken place at the surface, but cobalt and aluminum show active (percentage) decreasing trends (Table 4). It is likely that the tool is sharp and not heated and therefore no corrosion processes are active. The changes in the concentrations of the other elements between 3000 and 6000 m working distance can be described as insignificant, with the exception of a significant decrease in cobalt from 2.99 to 1.74% (active corrosion) and an increase in oxygen from 3.1 to 7.64% (active oxidation,

indicating the corrosive effect of corrosion on the tool). This indicates an increasing heating of the tool. The gradual decrease in cobalt concentration with increasing tool life indicates the increasing corrosive effect of intergranular crevice corrosion on this metal, which deteriorates the mechanical properties of the surface. The recovery of tungsten and cobalt concentrations between 6000 and 9000 m working distance indicates a change in the tungsten carbide grains on the surface. This is confirmed by the observed increase in surface roughness of the cutting edges as the weakly cobalt-bound tungsten carbide grains break away [35]. The significant decrease in oxygen content (1.28%) in this operating range indicates that the deep layers of the carbide were ‘opened’ by abrasion but not oxidized [35]. 9000 m is the limit of the quality performance of the tool: the surface layers of the WC grains have changed, the accuracy of the cutting edge deteriorates, the roughness of the tool increases, leading to an increase in the roughness of the surface to be machined, the energy required for machining increases and the tool heat increases.

3.2. Investigation of the Effect of Corrosion on WC-Co and Hard Coatings

The effect of the tannin solution on the optical image of the coatings at 20, 80 and 140 °C (exposure time 16h) is shown in Table 5.

Table 5. Effect of 16 h of tannin solution on the optical images of hard-metal WC-Co and PVD coatings at 20, 80 and 140 °C (×100).

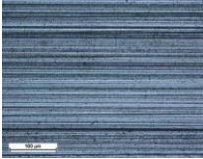
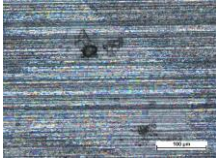
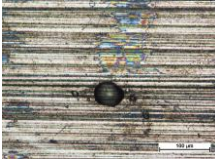
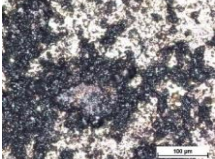
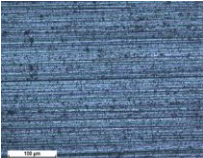
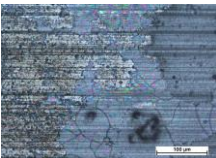
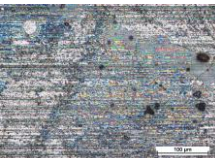
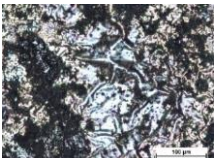
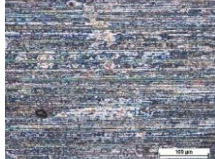
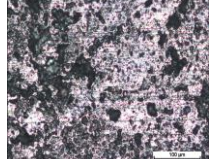
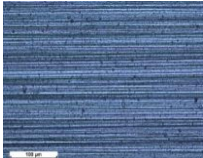
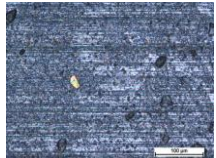
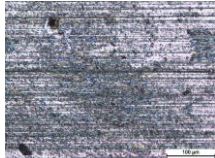
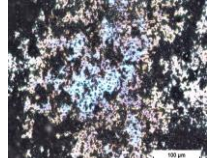
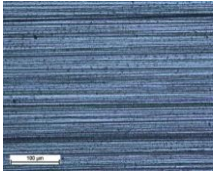
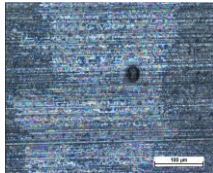
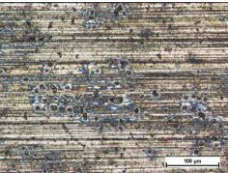
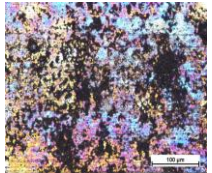
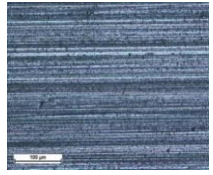
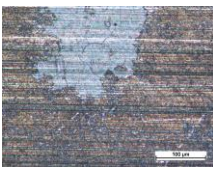
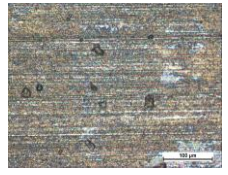
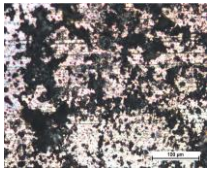
Material	Unproduced	Corroded at t, °C		
		20	80	140
WC-Co				
AlCrN				
AlTiN				
TiAlN				

Table 5. Cont.

Material	Unproduced	Corroded at t , °C		
		20	80	140
TiCN				
CrN				

Tannic acid $C_{76}H_{52}O_{46}$ solution at a concentration of 50 g/L in water at 20 and 80 °C caused pitting corrosion of the coatings, while the solution at 140 °C caused continuous corrosion damage in places (Table 5). The optically estimated pitting corrosion density is shown in Table 6. At a tannin solution temperature of 140 °C, about 30% of the CrN coating is affected by corrosion, while more than 50%–65% of the area is affected by the hard-metal WC-Co and other PVD coatings. The images presented in Table 5 show that the corrosion dynamics increase significantly at temperatures above 80 °C.

Table 6. Density of pitting corrosion on the surface of cutters at tannin solution temperatures of 20 and 80 °C.

Hard-Metal/PVD Coatings	Density of Pitting Corrosion Damage pcs/mm ²		Level of Corrosive Damage [37]	Corrosion Dynamics
	$t = 20$ °C	$t = 80$ °C		
WC-Co	23	37	Medium	Slightly increasing
AlCrN	12	44	Medium	Growing
AlTiN	5	5	Low	Not increasing
TiAlN	39	40	Medium	Not increasing
TiCN	4	121	High	Very fast
CrN	4	11	Low	Growing

The pitting corrosion densities and corrosion dynamics of the hard-metal WC-Co (without and with PVD coatings) at tannin solution temperatures of 20 and 80 °C are shown in Table 6.

At 20 °C, corrosion is most damaging to the TiAlN coating.

At temperatures of 20 and 80 °C, corrosion affected the AlTiN and CrN coatings the least (Table 6). The TiCN coating was most affected by corrosion. As the temperature of the corrosive medium increases, pitting corrosion tends to spread and become continuous over time.

At 140 °C, corrosion is particularly active—corrosion products “cover” the machining marks of the tool. According to Winkelmann [19], the corrosion dynamics change fundamentally at 60 °C.

It was found that (in the absence of a corrodible object in the medium, i.e., the cutting tool) at a temperature of 20 °C, the pH of the tannic acid solution is $pH_{(20\text{ °C})} = 3.74$;

$\text{pH}_{(80\text{ }^\circ\text{C})}=3.14$; $\text{pH}_{(140\text{ }^\circ\text{C})} = 2.87$, i.e., the acidity of the medium increases with increasing temperature. This is confirmed by the source [15]. The corrosive activity of the medium increases as the pH value decreases.

After the milling cutters had been in the tannic acid solution for 16 h, the chemical composition of the WC-Co and PVD coating surfaces was determined after cleaning (Table 7).

Table 7. EDS analysis of the surface composition of the samples before and after corrosion testing (mass %).

Hardmetal/PVD Coatings	Carbon (C)	Tungsten (W)	Cobalt (Co)	Oxygen (O ₂)	Aluminium (Al)	Nitrogen (N) ₂	Chromium (Cr)	Titanium (Ti)
WC-Co	5.01	88.1	4.3	2.1	-	-	-	-
WC-Co corroded	14.7	76.6	1.3	7.3	-	-	-	-
AlCrN	0.62	-	-	1.02	30.4	28.2	39.7	-
AlCrN corroded	8.6	-	-	6.1	32.2	20	33.2	-
AlTiN	0.29	-	-	6.01	24.7	29.6	-	39.4
AlTiN corroded	10.1	-	-	22.7	23.4	13.8	-	29.9
CrN	1.16	-	-	2.9	-	20.0	75.7	-
CrN corroded	2.4	-	-	3.4	-	17.7	70.2	-
TiAlN	0.38	-	-	1.24	19.8	31.3	-	47.3
TiAlN corroded	6.1	-	-	9.7	18.9	18.9	-	46.4
TiCN	6.45	-	-	0.62	-	13.5	-	79.4
TiCN corroded	7.6	-	-	17.0	-	1.0	-	74.3

Bold—high compositional change, not bold—low compositional change.

The corrosion change was evaluated by the increase in oxygen content on the surface of the analysis. The smallest changes were observed for CrN (2.9→3.4%), WC-Co (2.1→7.3%), AlTiN (6.01→22.7%), medium for AlCrN (1.02→6.1%), large for TiAlN (1.24→9.7%) and very high for TiCN (0.62→17.0%).

Coatings containing aluminum, chromium and titanium showed no significant changes in the corrosion behavior of these metals.

Tannic acid is known to activate the corrosion processes in the solid state [15,19]. This is confirmed by the 3.3-fold decrease in Co content on the WC-Co surface (Table 7). The absence of W and Co contents detected by EDS on the investigated surfaces of the PVD-coated blades can be explained by the high-quality homogeneous PVD coating with a thickness of 1.4–2 μm, the absence of mechanical attack and the shallow corrosion depths of tens/hundreds of nanometers.

The corrosion increased the carbon content of the hard-metal surface (WC-Co) (by a factor of 2.9) and the PVD coatings (up to a factor of 24.8). As with the hard coatings, this is most likely due to the reaction of the WC-Co and PVD coatings with the impurities in the tannic acid: Dextrin (C₆H₁₀O₅), Rubber (C₅H₈) and Disaccharide (C₁₂H₂₂O₁₁), and possibly to the tannic acid itself between the grains of WC-Co.

The surface composition results (Table 7) show that the oxygen content of the samples increases from 1.2 (CrN) to 27.4 (TiCN) times. This is most likely due to the reaction of the WC-Co and PVD coatings with impurities in the tannic acid: dextrin (C₆H₁₀O₅), disaccharide (C₁₂H₂₂O₁₁) and the sulfate class minerals alunite KAl₃(SO₄)₂(OH)₆, melanterite FeSO₄·7H₂O, jarosite KFe₃(SO₄)₂(OH)₆ and calcium chromate Ca(CrO₄) [38–40].

The aluminum content of TiAlN and AlTiN coatings decreases from 4.5 to 25.5% when the surfaces corrode. In contrast, the aluminum content of the AlCrN coating increased by 5.9%. This is probably due to the mineral alunite in the tannic acid solution $KAl_3(SO_4)_2(OH)_6$ [38].

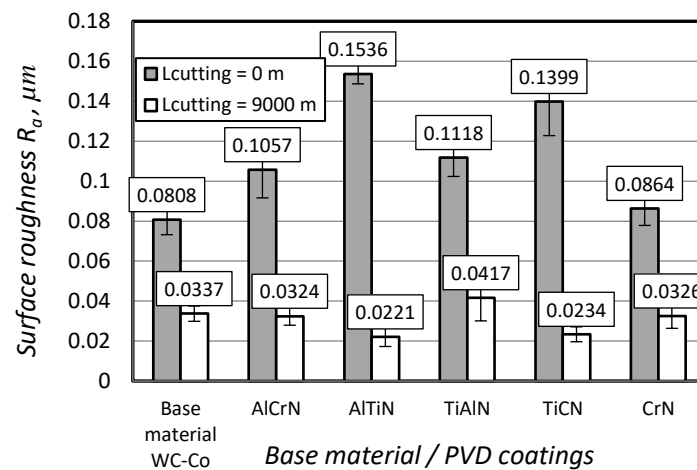
The corrosive effect of PVD coatings led to a 1.1 (CrN) to 13.5-fold (TiCN) reduction in the nitrogen content. In the case of chromium-containing coatings, corrosion reduced the chromium content by 7.27% in the CrN coating and 16.37% in the AlCrN coating. The corrosion reduced the titanium content in AlTiN, TiAlN and TiCN coatings by 29.5% (AlTiN), 24.11% (TiAlN) and 6.42% (TiCN).

3.3. Investigation of The effect of Tannin Acid on the Coefficient of Friction of Hard-Metal WC-Co and Hard Coatings

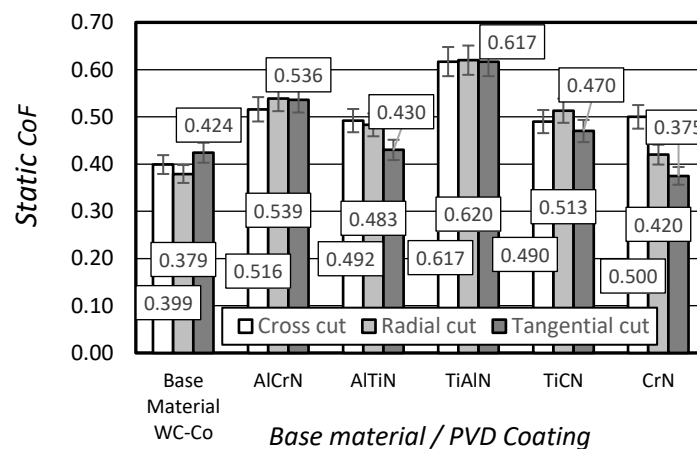
3.3.1. Static Coefficient of Friction

Since wood is a fibrous structural material, its hardness and other mechanical properties are different with respect to the fibers, and it is likely that the average static coefficient of friction (static CoF) is different in the different sections [41].

The roughness of the hard-metal and PVD coatings (new and after 9000 m of cutting) and the average static coefficients of friction (Static CoF) in the different wood sections (cross section, radial section, tangential section) are shown in Figure 8.



(a)



(b)

Figure 8. Roughness of hard-metal and hard coatings (a) [35] and the average static coefficients of friction (b) for different (cross cut, radial cut, tangential cut) wood sections.

The average static friction coefficients presented in Figure 8 show that the direction of the wood section does not significantly influence the static friction coefficient in the case of WC-Co and AlCrN, TiAlN, TiCN hard coatings. The direction of the cut has a statistically significant influence on the static friction coefficient only in the case of CrN, while in the case of the AlTiN coating the static friction coefficient is lower only in the tangential cut.

The fact that the coefficient of static friction of PVD-coated cutting tools is higher than the coefficient of friction of the substrate hard-metal WC-Co is also due to the fact that the roughness of the coated surface is higher in all cases [35].

3.3.2. Dynamic Coefficient of Friction

The average dynamic coefficients of friction determined perpendicular and parallel to the machining (grinding) direction of the cutters on the surfaces of not affected by corrosion hard-metal and PVD hard coatings are shown in Figure 9.

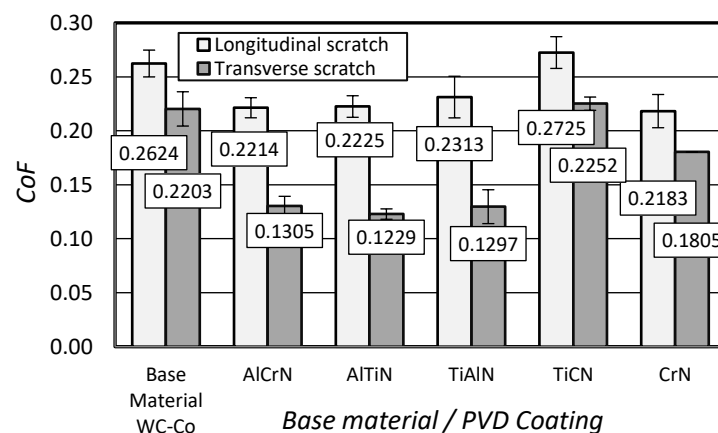


Figure 9. Coefficients of friction of WC-Co and PVD hard coatings parallel and perpendicular to the direction of grinding of the rake face of non-corroded cutters.

In all cases, the average coefficient of friction of non-corroded WC-Co and PVD hard coatings parallel to the machining direction is higher compared to the displacement perpendicular to the machining direction, ranging from 16.03% (WC-Co) to 44.8% (AlTiN coatings), Figure 9. It is evident that for the same indenter load and on surfaces with a sufficiently high surface smoothness ($R_a \approx 0.04 \mu\text{m}$), differences in the direction of the micro-relief lead to different contacts and surface stress fields (elastic deformation) in the indenter contact zone, which generate different resistance to movement forces.

It was found that the change in the composition of PVD coatings caused by the tannic acid significantly and systematically reduces the mechanical frictional forces between the indenter and the PVD coating surface: Figure 10 for the movement parallel to the machining direction, Figure 11 for the movement perpendicular to the machining direction. However, the extent to which the actual cutting process can be simulated (due to the dynamic processes of film formation and the degradation of corrosion products) can only be answered by direct precision measurement of the cutting forces.

The coefficient of friction between the indenter and the WC-Co treated with tannic acid decreases by 2.88%, while that of the PVD coatings decreases from 3.18% (for CrN) to 15.8% (for TiCN), Figure 10, indicating that the effect of the tannin solution changes the composition of the surface of the hard-metal and the coatings. It is quite logical that the CrN coating, which is the most corrosion resistant, had the least influence on the reduction of mechanical forces. The effect of the tannic acid solution on the surface of the tool materials (WC-Co and coatings) forms surface layers in the nanometer range, which probably have limited (lower mechanical) adhesion to the WC-Co or the hard coating material, so that the indenter slides more easily on the less mechanically resistant compounds. Therefore, the sliding resistance (coefficient of friction) test shows a lower coefficient of friction for

corroded surfaces, not in all cases with a statistically reliable difference, but with a clear downward trend.

It is likely that the highest decrease in friction coefficient (15.8% for TiCN) represents the most active corrosion susceptibility. This 2 μm thick coating showed the most severe wear in the cutting test.

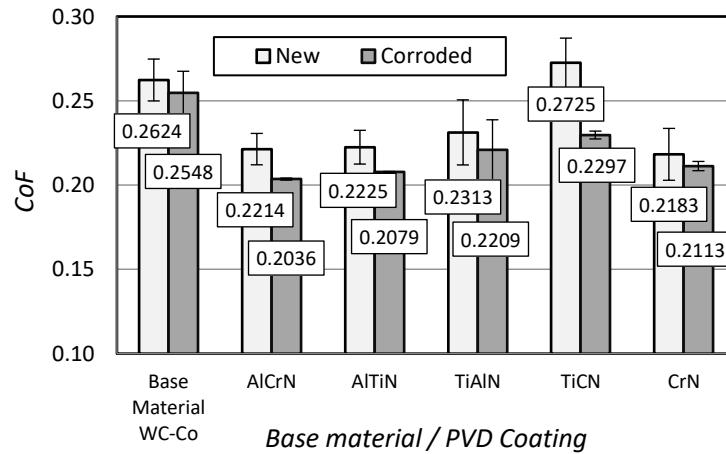


Figure 10. Average coefficient of friction between the indenter and the hard-metal WC-Co and PVD coatings on new and corroded samples parallel to the machining direction of the cutter.

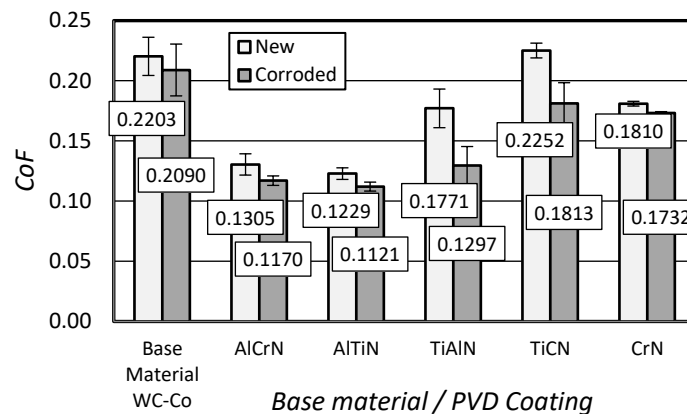


Figure 11. Average dynamic coefficient of friction between new and corroded hard-metal WC-Co and PVD coatings perpendicular to the machining direction of the cutter.

The dynamic coefficient of friction between WC-Co and WC-Co treated with tannic acid perpendicular to the machining direction is less than 5.13%. The displacement of the indenter in corroded PVD coatings is favored by a decrease in the coefficient of friction from 4.13% (for CrN) to 26.7% (for TiAlN).

The dynamic friction coefficients for samples exposed to corrosion perpendicular and parallel to the machining direction are shown in Figure 12.

At 140 °C and 5% concentration of the tannic acid solution, the friction coefficients of the surfaces of the samples concerned (parallel to the machining direction) are in all cases higher than the friction coefficient of the displacement perpendicular to the machining direction (Figure 12). The friction coefficient of the WC-Co hard-metal is 17.88% lower for the displacement perpendicular to the machining direction, while the friction coefficients of the PVD-coated samples are lower, ranging from 18.0% (CrN) to 46.1% (AlTiN).

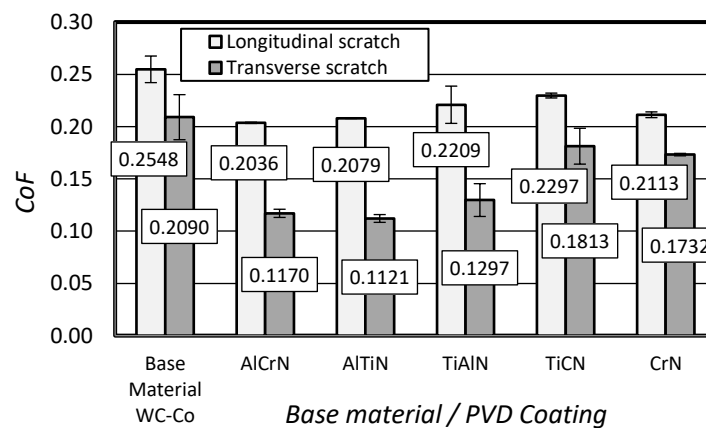


Figure 12. Dynamic coefficient of friction for displacement on corroded surfaces of WC-Co and PVD coatings in parallel and perpendicular to the machining directions of the cutter.

4. Discussion

Until now, tools for machining solid wood have been selected on the basis of their performance in machining metals. This approach ignored the combination of “wear-promoting” factors such as mechanical stress, temperature, friction and corrosion. In other words, the influence of these factors was not evaluated according to their importance. It is well known that there are significant differences between the mechanical properties of wood and metals and the temperatures generated at the tool cutting edges.

When using solid oak wood, which contains dominant extractive substances (tannic acid), it has been shown that corrosion during wood processing is a very important factor. In tools without PVD coating, corrosion of the cobalt binder of hard-metal WC-Co begins within the first few minutes of tool use. The tannic acid has the most intensive effect on the most sensitive part of the hard-metal—the cobalt, which binds the tungsten carbide grains. When most of the cobalt binder is removed from the WC grains (matrix), the majority of the cobalt grains become detached, resulting in changes to the cutting edge geometry, a loss of machining quality and increased energy consumption. However, the higher the cobalt content, i.e., the larger the intergranular layers of the cobalt matrix, the more active the corrosion. SEM analysis of the tools used shows that larger intergranular cobalt gaps on the surface lead to faster cobalt loss than smaller gaps. Therefore, hard-metals with lower binder concentrations have an advantage when machining solid wood. In addition, the dynamic effect on the tool are lower when machining solid wood compared to metal machining.

The aim of coating woodworking tools with PVD coatings is therefore to protect the hard-metal from corrosion for as long as possible. This should be achieved by looking for PVD coatings with potentially more resistant mechanical/abrasive wear properties for the respective wood species. For solid oak wood, these are chrome-containing PVD coatings—CrN and AlCrN. In a 120-min machining cycle from the cutting of the tool, these coatings with a thickness of 1.4–2.0 μm wear down to just 5 μm , minimizing the effects of corrosion on the hard-metal and machining quality.

PVD coatings protect the carbide of the tools from corrosive wear for as long as they are mechanically processed (abrasive wear) until they wear out.

A study of the dynamic coefficient of friction shows that in order to reduce machining costs for energy and tools, it is necessary to ensure that the sliding direction of the wood chips in the cutting tools and the finishing of the rake face of the cutter are perpendicular to each other.

5. Conclusions

Laboratory and production studies on the corrosion and tribological performance of hard-metal WC-Co cutters without and with PVD coatings led to the following conclusions:

1. The PVD coatings were worn away by mechanical (abrasive) wear and corrosion, and the tools had the following lifetimes: 6000 m for CrN and AlCrN; 3000 m for TiCN and TiAlN, and 2000 m for AlTiN.
2. Tannic acid solution in water (50 ml) at 20, 80 °C causes pitting corrosion of hard-metal and solid PVD coatings; at a solution temperature of 140 °C, about 30% of the surface of CrN coating is corroded in 16 h, and 50%–65% of the surface of WC-Co and other PVD coatings are affected.
3. Machining solid oak wood leads to intercrystalline corrosion of the WC-Co binder (cobalt) of the cutter, while corrosion of the PVD-coated tool base begins if the coating does not remain under the influence of abrasive wear. The less resistant the PVD coating is to mechanical (abrasive) wear, the earlier the corrosive effect on the cutter's hard-metal matrix (cobalt) begins. The corrosion causes the surface grains (WC) of the hard-metal alloy to break away after the loss of mechanical strength;
4. The direction of the wood cut has no real influence on the static coefficient of friction for WC-Co hard-metal and PVD hard coatings on tools.

Dynamic coefficient of friction:

- The increase with movement in parallel machining direction compared to perpendicular movement is between 16.03% (WC-Co) and 44.8% (AlTiN coating);
 - Decrease in tannic acid treatment of WC-Co (2.88%) and PVD coating on the surface from 3.18 (CrN) to 15.8% (TiCN).
5. Finishing operations on cutting tools perpendicular to the sliding direction of the chip reduce the coefficient of friction (ranging from 16.03%, WC-Co to 44.8%, AlTiN coatings), between the tool and the chip, which reduces the energy required for machining.

Author Contributions: Conceptualization, D.K. and V.J.; methodology, V.J.; software, M.A.; validation, D.K. and V.J.; formal analysis, D.K.; investigation, D.K.; resources, D.K. and V.J.; data curation, D.K. and V.J.; writing—original draft preparation, D.K. and V.J.; writing—review and editing, D.K. and V.J.; visualization, D.K. and V.J.; supervision, V.J.; project administration, D.K. and V.J.; All authors have read and agreed to the published version of the manuscript.

Funding: This research received no external funding.

Institutional Review Board Statement: Not applicable.

Informed Consent Statement: Not applicable for studies not involving humans.

Data Availability Statement: Data are contained within the article.

Conflicts of Interest: The authors declare no conflict of interest.

References

1. Bodîrlău, R.I.; Spiridon, C.A. Teacă, Chemical investigation of wood tree species in temperate forest in east-northern Romania. *BioResources* **2007**, *2*, 41–57. [[CrossRef](#)]
2. Bjurhager, I.; Berglund, L.A.; Bardage, S.L.; Sundberg, B. Mechanical characterization of juvenile European aspen (*Populus tremula*) and hybrid aspen (*Populus tremula* × *Populus tremuloides*) using full-field strain measurements. *J. Wood Sci.* **2008**, *54*, 349–355. [[CrossRef](#)]
3. Merela, M.; Čufar, K. Gustoća i mehanička svojstva drva bjeljike hrasta u usporedbi s drvom srži (Gustoća and mechanical properties of oak firewood in relation to srži firewood). *Drv. Ind.* **2013**, *64*, 323–334. [[CrossRef](#)]
4. Lica, D.; Coşoreanu, C. Investigation on the Properties of Pedunculate Oak Wood Affected By Oak Decline. *Pro Ligno* **2014**, *10*, 69–98.
5. Vilkovská, T.; Klement, I.; Výbohová, E. The effect of tension wood on the selected physical properties and chemical composition of beech wood (*Fagus sylvatica* L.). *Acta Fac. Xylologiae* **2018**, *60*, 31–40. [[CrossRef](#)]
6. Andrade, F.W.C.; Filho, M.T.; Moutinho, V.H.P. Influence of wood physical properties on charcoal from *Eucalyptus* spp. *Floresta e Ambiente* **2018**, *25*, e20150176. [[CrossRef](#)]
7. Ištók, I.; Sedlar, T.; Šefc, B.; Sinković, T.; Perković, T. Physical properties of the firewood of the clonal poplar trees I'-214' and S'1-8'. *Drv. Ind.* **2016**, *67*, 163–170. [[CrossRef](#)]

8. Martínez-Cabrera, H.I.; Jones, C.S.; Espino, S.; Jochen Schenk, H. Wood anatomy and wood density in shrubs: Responses to varying aridity along transcontinental transects. *Am. J. Bot.* **2009**, *96*, 1388–1398. [[CrossRef](#)] [[PubMed](#)]
9. Maiti, K.A.; Rodriguez, R.H.G. Wood Density of Ten Native Trees and Shrubs and Its Possible Relation with a Few Wood Chemical Compositions. *Am. J. Plant Sci.* **2016**, *7*, 1192–1197. [[CrossRef](#)]
10. Pásztor, Z.; Börcsök, Z.; Ronyecz, I.; Mohácsi, K.; Molnár, S.; Kis, S. Oven dry density of sessile oak, Turkey oak and hornbeam in different region of Mecsek Mountain. *Wood Res.* **2014**, *59*, 683–694.
11. Kazlauskas, D.; Jankauskas, V. Woodworking tools: Tribological problems and directions of solutions. In Proceedings of the 9th International Conference BALTRIB, Kaunas, Lithuania, 16–17 November 2018; pp. 178–187. [[CrossRef](#)]
12. Goodrich, T.; Nawaz, N.; Feih, S.; Lattimer, B.Y.; Mouritz, A.P. High-temperature mechanical properties and thermal recovery of balsa wood. *J. Wood Sci.* **2010**, *56*, 437–443. [[CrossRef](#)]
13. Gibson, L.J. The hierarchical structure and mechanics of plant materials. *J. R. Soc. Interface* **2012**, *9*, 2749–2766. [[CrossRef](#)] [[PubMed](#)]
14. Cabane, E.; Keplinger, T.; Künniger, T.; Merk, V.; Burgert, I. Functional lignocellulosic materials prepared by ATRP from a wood scaffold. *Sci. Rep.* **2016**, *6*, 31287. [[CrossRef](#)] [[PubMed](#)]
15. Zelinka, S.L.; Stone, D.S. The effect of tannins and pH on the corrosion of steel in wood extracts. *Mater. Corros.* **2011**, *62*, 739–744. [[CrossRef](#)]
16. Tondi, G.; Thevenon, M.F.; Mies, B.; Standfest, G.; Petutschnigg, A.; Wieland, S. Impregnation of Scots pine and beech with tannin solutions: Effect of viscosity and wood anatomy in wood infiltration. *Wood Sci. Technol.* **2013**, *47*, 615–626. [[CrossRef](#)]
17. Darmawan, W.M.R.; Rahayu, I.; Nandika, D. The importance of extractives and abrasives in wood materials on the wearing of cutting tools. *BioResources* **2012**, *7*, 4715–4729. [[CrossRef](#)]
18. Darmawan, W.M.R.; Rahayu, I.; Nandika, D. Wear characteristics of wood cutting tools caused by extractive and abrasive materials in some tropical woods. *J. Trop. For. Sci.* **2011**, *23*, 345–353.
19. Winkelmann, H.; Badisch, E.; Roy, M.; Danninger, H. Corrosion mechanisms in the wood industry, especially caused by tannins. *Mater. Corros.* **2009**, *60*, 40–48. [[CrossRef](#)]
20. Winkelmann, H.E.S.; Badisch, E.; Ilo, S. Corrosion Behaviour of Tool Steels in Tannic Acid. *Mater. Corros.* **2009**, *60*, 192–198. [[CrossRef](#)]
21. Etele Csanády, E. *Mechanics of Wood Machining*, 2nd ed.; Department of Wood Engineering, University of West Hungary: Sopron, Hungary, 2011. [[CrossRef](#)]
22. De Lacalle, L.N.L.; Fernández-Larrinoa, J.; Rodríguez-Ezquerro, A.; Fernández-Valdivielso, A.; López-Blanco, R.; Azkona-Villaverde, I. On the cutting of wood for joinery applications. *Proc. Inst. Mech. Eng. Part B J. Eng. Manuf.* **2015**, *229*, 940–952. [[CrossRef](#)]
23. Varga, M.; Winkelmann, H.; Badisch, E. Impact of microstructure on high temperature wear resistance. *Procedia Eng.* **2011**, *10*, 1291–1296. [[CrossRef](#)]
24. Kazlauskas, D.; Keturakis, G. Investigation of wear resistance of router cutters coated different antiwear coatings. In *Proceedings of the Innovative (Eco-) Technology, Entrepreneurship and Regional Development*; Kaunas University of Technology: Kaunas, Lithuania, 2015; ISBN 978-9955-27-479-9.
25. Kazlauskas, D.; Jankauskas, V.; Tuckute, S. Research on tribological characteristics of hard metal WC-Co tools with TiAlN and CrN PVD coatings for processing solid oak wood. *Coatings* **2020**, *10*, 632. [[CrossRef](#)]
26. Kazlauskas, D.; Jankauskas, V.; Keturakis, G. Research on durability of AlCrN coated tungsten carbide (WC-Co) cutters during oakwood milling. In Proceedings of the The 10th International Conference BALTRIB'2019, Akademija, Kaunas, Lithuania, 14–16 November 2019; pp. 243–249. [[CrossRef](#)]
27. Liu, Z.; Ren, S.; Li, T.; Chen, P.; Hu, L.; Wu, W.; Li, S.; Liu, H.; Li, R.; Zhang, Y. A Comparison Study on the Microstructure, Mechanical Features, and Tribological Characteristics of TiN Coatings on Ti6Al4V Using Different Deposition Techniques. *Coatings* **2024**, *14*, 156. [[CrossRef](#)]
28. Yan, W.; Li, C.; Liu, Z.; Cheng, C.; Yang, L. Reliability Evaluation of EB-PVD Thermal Barrier Coatings in High-Speed Rotation and Gas Thermal Shock. *Coatings* **2024**, *14*, 136. [[CrossRef](#)]
29. Kowalski, S.; Pexa, M.; Aleš, Z.; Čedík, J. Failure analysis and the evaluation of forced-in joint reliability for selected operation conditions. *Coatings* **2021**, *11*, 1305. [[CrossRef](#)]
30. Tabakov, V.P.; Vereschaka, A.S.; Vereschaka, A.A. Multilayer composition coatings for cutting tools: Formation and performance properties. *Mech. Ind.* **2017**, *18*, 706. [[CrossRef](#)]
31. Liu, Y.; Yu, S.; Shi, Q.; Ge, X.; Wang, W. Multilayer Coatings for Tribology: A Mini Review. *Nanomaterials* **2022**, *12*, 1388. [[CrossRef](#)]
32. Cezar, H.; Jambo, M.; Szogyenyi, A.; Pukasiewicz, A.G.M.; Biava, G.; Fernandes Siqueira, I.B.A.; Vaz, R.F.; Biscaia de Souza, G. Evaluation of high temperature corrosion resistance of CrN, AlCrN, and TiAlN. *Surf. Coat. Technol.* **2022**, *438*, 128398.
33. Ghorbani, A.; Elmkhah, H.; Imantalab, O.; Meghdari, M.; Nouri, M.; Fattah-alhosseini, A. The impact of mechanical post-treatment on the tribological and corrosion behavior of CrN/CrAlN coatings applied using the CAE-PVD technique. *Appl. Surf. Sci. Adv.* **2023**, *18*, 100477. [[CrossRef](#)]
34. Tools Cut Better with TIGRA, (n.d.). Available online: https://www.tigra.de/fileadmin/user_upload/PDF/2018/Woodworking2019.pdf (accessed on 30 March 2024).

35. Kazlauskas, D.; Jankauskas, V.; Kreivaitis, R.; Tučkutė, S. Wear behaviour of PVD coating strengthened WC-Co cutters during milling of oak-wood. *Wear* **2022**, *498*, 204336. [[CrossRef](#)]
36. Kurlov, A.I.G.A.S. Fizika i Chimija Karbidov Volframa. Fizmatlit 2014. pp. 182–193, ISBN 978-5-9221-1477-6. Available online: <https://www.labirint.ru/books/509994/> (accessed on 30 March 2024).
37. ISO 4628-3; Paints and Varnishes—Evaluation of Degradation of Coatings—Designation of Quantity and Size of Defects, and of Intensity of Uniform Changes in Appearance—Part 3: Assessment of Degree of Rusting. International Organization for Standardization: Geneva, Switzerland, 2016; p. 4628.
38. Zimbelman, D.R.; Rye, R.O.; Breit, G.N. Origin of secondary sulfate minerals on active andesitic stratovolcanoes. *Chem. Geol.* **2005**, *215*, 37–60. [[CrossRef](#)]
39. Lacalamita, M.; Ventruti, G.; Della Ventura, G.; Radica, F.; Mauro, D.; Schingaro, E. In situ high-temperature x-ray powder diffraction and infrared spectroscopic study of melanterite, $\text{FeSO}_4 \cdot 7\text{H}_2\text{O}$. *Minerals* **2021**, *11*, 392. [[CrossRef](#)]
40. Lee, Y.M.; Nassaralla, C.L. Standard free energy of formation of calcium chromate. *Mater. Sci. Eng. A* **2006**, *437*, 334–339. [[CrossRef](#)]
41. Desch, J.M.D.H.E. *Timber: Structure, Properties, Conversion and Use*, 7th ed.; Food Products Press: New York, NY, USA, 1996.

Disclaimer/Publisher’s Note: The statements, opinions and data contained in all publications are solely those of the individual author(s) and contributor(s) and not of MDPI and/or the editor(s). MDPI and/or the editor(s) disclaim responsibility for any injury to people or property resulting from any ideas, methods, instructions or products referred to in the content.